

# DeCoF: Generated Video Detection via Frame Consistency

Long Ma<sup>†1</sup> Jiajia Zhang Hongping Deng Ningyu Zhang Yong Liao Haiyang Yu<sup>†</sup>

## Abstract

The escalating quality of video generated by advanced video generation methods leads to new security challenges in society, which makes generated video detection an urgent research priority. To foster collaborative research in this area, we construct the first open-source dataset explicitly for generated video detection, providing a valuable resource for the community to benchmark and improve detection methodologies. Through a series of carefully designed probe experiments, our study explores the significance of temporal and spatial artifacts in developing general and robust detectors for generated video. Based on the principle of video **frame consistency**, we introduce a simple yet effective **detection model (DeCoF)** that eliminates the impact of spatial artifacts during generalizing feature learning. Our extensive experiments demonstrate the efficacy of DeCoF in detecting videos produced by unseen video generation models and confirm its powerful generalization capabilities across several commercial proprietary models.

## 1. Introduction

Following the success of diffusion models in generating highly realistic images (Nichol & Dhariwal, 2021; Rombach et al., 2022; Parmar et al., 2023), a growing number of researchers have shifted their focus to the advancement of these models for video generation (Kawar et al., 2023; Blattmann et al., 2023; Zhang et al., 2023). Such developments have turned diffusion models into robust and versatile video generators, enabling the creation of high-quality videos from general conditional inputs, such as text and images. While this powerful and flexible generation capacity has the potential to alleviate the stress of daily life and inspire creativity in work, it concurrently introduces a new crisis of trust (Sharma et al., 2023; Barrett et al., 2023). Therefore, there is an urgent need for detectors capable of

<sup>†</sup>Department of Cyberspace Security, University of Science and Technology of China, Hefei, China. Correspondence to: Long Ma <longm@mail.ustc.edu.cn>.

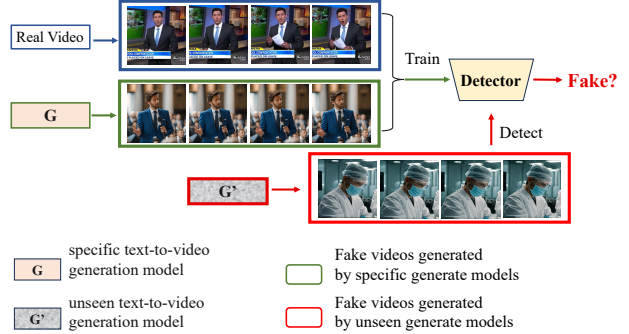


Figure 1. Can the detector trained on a specific video generation model cope with the challenges presented by unseen generation models?

identifying generated videos.

In this paper, we propose a challenging task: **Generated Video Detection**, which aims to create universal detectors to deal with the trust crisis caused by various emerging text-to-video (T2V) models, especially unseen models. To evaluate generated video detectors, we create the first comprehensive generated video detection dataset: the *GeneratedVideoForensics* (GVF) dataset. The GVF dataset encompasses a wide range of scene contents and motion variations, approximating the authenticity verification problem caused by the T2V generation model in diverse actual environments. Moreover, pairs of real and generated videos in the dataset are constructed using the same prompt to ensure that the generated video detectors learn subtle distinctions to identify the authenticity of videos rather than learning differences between the content of the real and fake videos. Furthermore, we construct generated samples corresponding to real videos based on various T2V models with different generation methods and model architectures (Khachatryan et al., 2023; Zhang et al., 2023; Wang et al., 2023a; Sterling, June 2023), such as pixel-space or latent-space models, which aims to measure the generality of the generated video detectors.

Considering that video content contains individual frame contents and smooth consistency across multiple frames, a natural idea is to utilize end-to-end spatiotemporal convolutional neural networks (STCNN) models to achieve

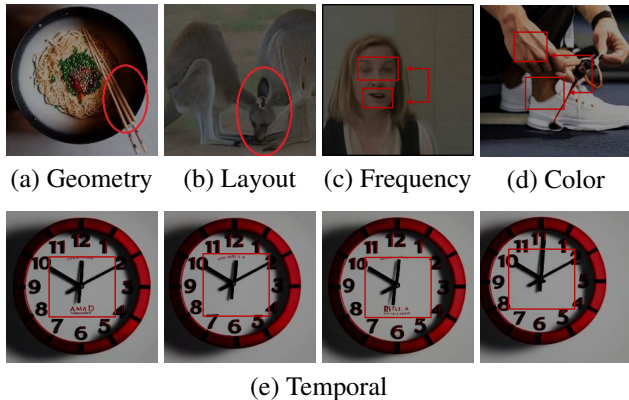


Figure 2. **Spatial and temporal artifacts on generated video.** We illustrate the spatial and temporal artifacts present in the generated videos. Spatial artifacts: (a) errors in geometric appearance, (b) errors in image layout, (c) frequency inconsistency, (d) color mismatch; Temporal artifacts: (e) mismatch between frames.

generated video detection. Our exploratory experiments found that these models have excellent discriminative capabilities for specific T2V models but cannot be applied to detect unseen T2V models. Further probe experiments in Table 1 reveal that the spatiotemporal convolutional models predominantly identify video authenticity by detecting spatial artifacts, resulting in generated video detection that has degenerated into a 2D problem. A critical question arises: **Spatial and temporal artifacts, which artifacts are key to constructing universal detectors?**

To explore this problem, we first analyze the possibility of building a universal generated video detector through spatial artifacts. We convert the 3D problem of generated video detection into a 2D problem, generated image detection, and implement T2V detection based on existing text-to-image (T2I) detection methods. In section 5.2, we evaluate the performance of these generated image detectors on generated video detection, noting that the reason why these detectors lack generality to unseen generative models is that capturing specific spatial artifacts to identify video authenticity, while spatial artifacts are specific to the T2V model, these detectors are unable to capture more general and high-level spatial artifacts to establish better decision boundaries. So far, we conclude that spatiotemporal convolutional models primarily identify video authenticity by detecting spatial artifacts but are unable to detect more general spatial artifacts. **Since spatial artifacts are easily detected, learning of temporal artifacts is difficult to perform.**

To rectify this biased learning approach, mitigate the adverse effects induced by spatial artifacts, and construct a more generalizable generated video detector by capturing temporal artifacts, we propose to decouple temporal and spatial artifacts by mapping video frames to feature space, where

the distance between features is negatively correlated with image similarity, through a pre-trained CLIP:ViT (Dosovitskiy et al., 2020). More importantly, the features of real video frames are still continuous after being mapped by the mapping function with the above requirements. Meanwhile, the frames of the generated video with inter-frame mismatch will have anomalies in their features. Besides, it greatly reduces computational complexity and memory requirements since only anomalies between features need to be learned. Specifically, we only implement the learning of inter-feature anomalies through a temporal artifact modeling module with two transformer layers (Vaswani et al., 2017). Extensive exploring experiments demonstrate that our method exhibits extraordinary capabilities in generated video detection, especially significant generalization capabilities for unseen generation models.

Our contributions are summarized as follows:

- We present the first dataset that is comprehensive and scalable as new models emerge for benchmarking generated video detectors.
- We explore the possibility of detecting generated videos by capturing spatial and temporal artifacts and point out the drawbacks of the detector by capturing spatial artifacts and their causes.
- We develop a universal generated video detector named DeCoF, validating through extensive experiments, including tests on commercial proprietary models.

## 2. Related work

### 2.1. Generation Models

Recently, with the success of diffusion models in generating images (Ho et al., 2020; Song et al., 2020; Nichol & Dhariwal, 2021; Esser et al., 2021; Rombach et al., 2022; Peebles & Xie, 2023), a number of Research explores text-to-video Diffusion Models (VDMs). Some work (Ramesh et al., 2022; Blattmann et al., 2023; Khachatryan et al., 2023; Wang et al., 2023a) ground their models on latent-based VDMs, for example, Text2Video-zero (Khachatryan et al., 2023) generates videos by using motion dynamics to enhance the latent code of a text-to-image stable diffusion model without requiring training on any video data, and ModelScopeT2V (Wang et al., 2023a) extends it with T2I stable diffusion model of convolutional and attentional blocks and trained using image-text and video-text datasets, ZeroScope (Sterling., June 2023) is a watermark-free T2V generative model trained with the weights of ModelScopeT2V, which is optimized for 16:9 compositions. On the other hand, PYoCo (Ge et al., 2023) and Make-A-Video (Singer et al., 2022) anchor their models on pixel-based VDMs. Show1 (Zhang et al., 2023) integrates pixel-

based and latent-based VDMs, using Pixel-based VDMs to produce videos of lower resolution with better text-video alignment, while latent-based VDMs upscale these low-resolution videos from pixel-based VDMs to then create high-resolution videos with low computation cost.

## 2.2. Generated Content Detections

In recent years, a large amount of work has focused on generated image detection (McCloskey & Albright, 2019; Zhang et al., 2019; Barni et al., 2020; Corvi et al., 2023; Sha et al., 2023), especially for unseen generation models. A simple classifier trained by Wang et al. (Wang et al., 2020) on pagan-generated images using multiple data augmentations can be generalized to 20 unseen other GAN-generated images. Frank et al. (Frank et al., 2020) concluded that the artifacts of the generated images are caused by the upsampling method. Wang et al. (Wang et al., 2023b) identify generated images through the difference of images reconstructed by a pre-trained diffusion model. Tan et al. (Tan et al., 2023) adopt a pre-trained CNN model as transformation models convert images into gradients. Ojha et al. (Ojha et al., 2023) proposed based on pre-trained vision-to-language models to develop a universal generated image detector. In orthogonal, a large amount of work focuses on the detection of Deepfake images (Guarnera et al., 2020; Li et al., 2020; Zhao et al., 2021a; Shiohara & Yamasaki, 2022), such as artificially creating general forged boundaries (Shiohara & Yamasaki, 2022), detect shifts in the frequency domain (Guo et al., 2023), and detect Deepfake from inconsistencies in face image regions (Zhao et al., 2021b).

So far, there are some studies on detecting Deepfake videos (Güera & Delp, 2018; Masi et al., 2020; Agarwal et al., 2020; Haliassos et al., 2021; Wang et al., 2023c), but there is a lack of research specifically focused on detecting generated videos. We hope this paper can bring exploratory and insightful contributions to this domain of study.

## 3. Problem Formulation

**Generated Video Detection.** In addition to the generalization ability of generated video detectors to unseen generation models, we also focus on the generalization to cross-category videos. So, the generated video detection task is defined as follows:

Given a collection of real videos denoted as  $R = \{r_1, r_2, \dots, r_n\}$ , a set of content prompts  $P = \{p_1, p_2, \dots, p_n\}$ , where  $r_i$  and  $p_i$ ,  $i \in [1, n]$  refers to each real video and its corresponding content prompt. And let  $G = \{g_1, g_2, \dots, g_m\}$  denotes video generation models, where  $g_j$ ,  $j \in [1, m]$  represents a specific video generation model. Accordingly, based on the prompt  $p_i$  of each real video  $r_i$ , it generates  $m$  corresponding

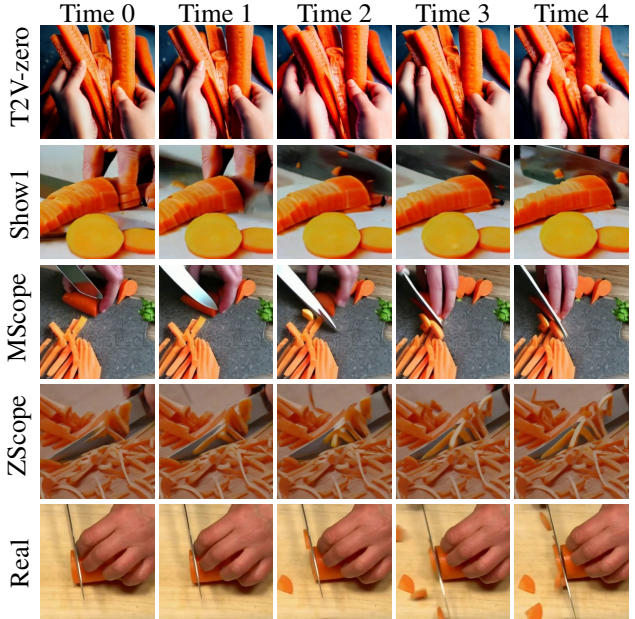


Figure 3. We generated four sub-datasets based on the prompts of real videos and generation models based on four different architectures and generation methods: Text2Video-zero, ModelScopeT2V, ZeroScope, and SHOW-1. Each pair of positive and negative samples follows the same prompt, and we show the first five frames of four pairs of positive and negative samples corresponding to one of the prompts: **A person is cutting a carrot.**

generated videos, resulting in a set of fake video collections  $F_j \in F = \{F_1, F_2, \dots, F_m\}$ , where  $F_j = \{g_j(p_1), g_j(p_2), \dots, g_j(p_n)\}$ . the generated video detection dataset  $D_j \in \mathcal{D} = \{D_1, D_2, \dots, D_m\}$ , where  $D_j = \{(x, y)^{(i)}\}_{i=1}^n$ , with  $x \in \mathcal{X} = \{R, F_j\} \subset \mathbb{R}^{L \times H \times W \times C}$  and  $y \in \mathcal{Y} = \{0, 1\}$  denoting a video and its label,  $L, H, W$  and  $C$  correspond to the video length, video frame height, width and number of channels, respectively.

The goal of generated video detection is to train a detector  $\mathcal{F}$  on a subdataset  $D_j$  built based on a known generate model  $m_j$ , map the video space to the category space  $\mathcal{F} : \mathcal{X} \rightarrow \mathcal{Y}$ , and achieve generalization on unseen generate models  $g_k$ , where  $k \in [1, m], k \neq j$ . This can be achieved by minimizing classification error of  $\mathcal{F}$  on training data  $D_i^*$ :

$$\arg \min_{\theta} \mathbb{E}_{(x,y) \in D_i^*} \mathcal{L}(f(x), y) \quad (1)$$

Where  $\mathcal{L}$  is a loss function, and  $\theta$  are the trainable parameters of detector  $f$ ,  $D_i^*$  refers to the training set of  $D_i$ . We implement the evaluation of detection of cross-category generated videos by ensuring that the training set and the test set do not have videos with the same prompt.

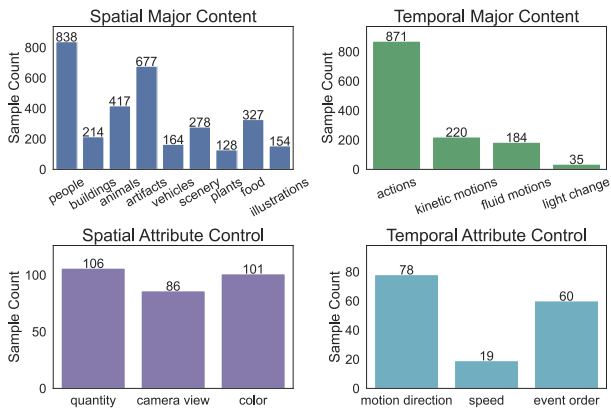


Figure 4. Data distribution over categories under the “major content (upper) and “attribute control” (lower) aspects.

## 4. Dataset Construction

To benchmark generated video detectors, we created the first dataset for the generated video detection task: the *GeneratedVideoForensics* dataset. In this section, we mainly introduce the construction of the data set and conduct a comprehensive evaluation of the dataset.

### 4.1. Dataset Composition

The *GeneratedVideoForensics* (GVF) dataset  $\mathcal{D}$  consists of 964 triples and can be represented as  $\mathcal{D} = \{(R, P, F)^{(i)}\}_{i=1}^{964}$ ,  $R$  and  $P$  represent the real video and the corresponding text prompt, and  $F$  represents multiple fake videos generated by different generation models based on the text prompt  $P$ . In order to examine the generalization of the detectors, we selected four open source generate models with different generation methods and model frameworks: Text2Video-zero (Khachatryan et al., 2023), ModelScopeT2V (Wang et al., 2023a), ZeroScope (Sterling, June 2023) and SHOW-1 (Zhang et al., 2023) as generation models for negative samples. Therefore, the GVF dataset could be divided into four sub-datasets: Text2Video-zero, ModelScopeT2V, ZeroScope, and Show1. Figure 3 shows an example of one of the triples.

**Prompt.** To approximate the distribution of videos in real task scenarios, we collected 964 prompts and corresponding real videos from existing open-domain text-to-video datasets: MSVD (Chen & Dolan, 2011) and MSR-VTT (Xu et al., 2016) datasets. Following the FTEV (Liu et al., 2023), we consider the collection of prompts from the following four aspects to simulate the sample distribution in real scenarios: the spatial and temporal major content it describes and the spatial and temporal attributes it controls during video generation. Spatial content is classified as people, animals, plants, food, vehicles, buildings, and artifacts, with corresponding spatial attributes of quantity, color, and cam-

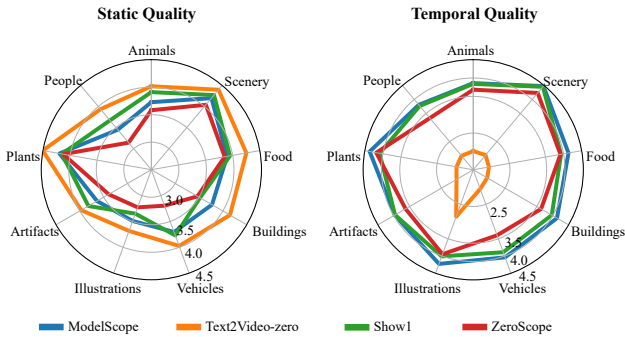


Figure 5. Manual evaluation results across spatial major contents.

era view. Temporal content and attributes encompass actions, kinetic motions, fluid motions, and light change, with attributes including motion direction, speed, and event order. This ensures that our data set is comprehensive and balanced. Figure 4 shows the data distribution on categories under different aspects, which shows that the GVF dataset contains enough data to cover different category ranges.

### 4.2. Dataset Evaluation

Among many excellent T2V generation models, we have selected four of the most representative open-source models, including different generation ideas and model architectures, to restore better the challenges posed by invisible generation models. Figure 5 shows the performance of videos generated by the above four generation models on different attributes under the FETV (Liu et al., 2023) standard. In order to generate different kinds of content, it is obvious to note that each of these models has its advantages and disadvantages. Text2Video-zero, for example, has the best impact on the spatial quality of the video but the worst impact on the temporal continuity. On the contrary, ZeroScope has a better effect on temporal continuity but has the worst effect on spatial quality. The choice of these video generation models, each possessing distinct advantages and disadvantages, ensures that our dataset can effectively measure the performance of detectors when facing unseen T2V generation models.

## 5. Methodology

### 5.1. Probe experiments of STCNN models

Initially, we considered using a spatiotemporal convolutional model (STCNN) to train the generally generated video detector. However, we discovered that these models are only effective on the specific generative models they were trained on and needed more generalizability, failing to discern unseen T2V generation models.

To analyze what information the STCNN network was learn-

Table 1. Spatiotemporal Convolutional Neural Networks (3DCNN) rely on easily detectable spatial artifacts.

Method	Artifacts				Difference	
	Temporal		Spatial		ACC	AP
	ACC	AP	ACC	AP		
I3D	51.17	51.61	86.67	98.61	35.50	47.00
Slow	50.04	50.37	93.81	99.51	43.77	49.14
X3D	50.04	54.31	78.39	92.84	28.35	38.53
Mvit	50.48	55.29	72.16	92.59	21.68	37.30

ing during discrimination, or rather, which features within the video it was utilizing to distinguish between authentic and fabricated content, we designed a sophisticated probe experiment with two novel datasets under the same model framework: The first dataset involves scrambling the frames of all real videos in the current test set, destroying the temporal continuity of the videos, to see if the model can still differentiate based solely on the temporal discontinuities of the videos. The second dataset was created by randomly selecting a frame from the current test set and replicating it multiple times to see if the model could still differentiate based on the spatial artifacts of the video frame alone.

The experimental results in table 1 led us to the following conclusion: We found that the model’s attention to spatial artifacts and temporal artifacts was distinct, and for developing a generalized discriminator, they did not play the same role. Therefore, we attempt to build detectors based on spatial artifacts and temporal artifacts separately, individually verifying the role each played in the learning process of the universally generated video detector.

## 5.2. Shortcomings of learning from spatial artifacts

To analyze the role of spatial artifacts, we first work with existing T2I models which have been used as image-level detectors for generated videos, and we test them on the GVF dataset. As shown in Table 2, these detectors demonstrate superior capabilities in capturing the spatial artifacts of specific generation models. However, they lack generalization to unseen generation models.

To find out why these detectors lack generalization to unseen generate models, we visualized the feature space of the detector (Wang et al., 2020) and examined the distribution of four sub-datasets: (i) Real, comprising real videos from the test set, (ii) T2V, consisting of fake videos from the sub-dataset Text2Video-zero, (iii) Show1, composed of fake videos from the sub-dataset Show-1, and (iv) MP, comprised of fake videos from the sub-dataset ModelScope, (v) ZP, comprised of fake videos from the sub-dataset ZeroScope. For each video, we utilized the detector trained on (i) and (ii) to extract their feature representations corresponding

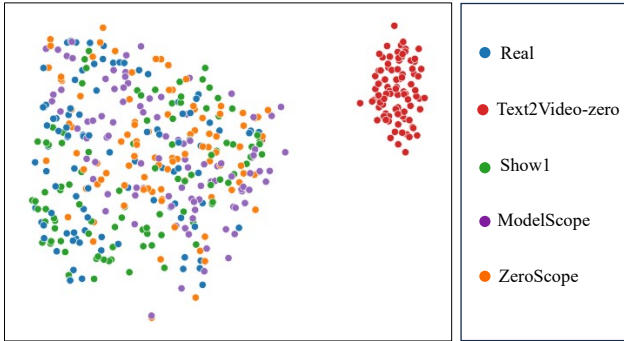


Figure 6. t-SNE visualization of real and fake video frames associated with four video generation models. The feature space used is one trained to distinguish fake videos (Text2Video-zero) from real videos.

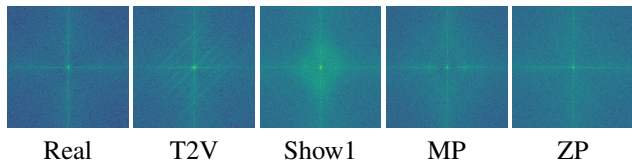


Figure 7. Average spectrum of video frames for real videos and fake videos generated by different video generation models.

to each frame and subsequently visualized these through t-SNE (Van der Maaten & Hinton, 2008).

As shown in Figure 6, on the one hand, the detector has ideally classified the real video and the fake video generated by the specific generate model, which means that the detector has fully captured the spatial artifacts of the specific generate model Text2Video-zero (Khachatryan et al., 2023). On the other hand, the detector cannot distinguish fake videos generated by unseen models from real videos. Why are the spatial artifacts captured by the detector in (ii) not helpful for detecting other video generation models? We illustrate this by visualizing the frequency spectrum of video frames generated by various video generate models. As shown in Figure 7, although the generated videos all have spatial artifacts, such as parallel slashes appearing in T2V and bright spots appearing in Show-1, these spatial artifacts are not consistent; capturing more general spatial artifacts appears to be extremely difficult.

## 5.3. Eliminate impact of spatial artifacts

There is no doubt that real video frames are continuous, and we can even predict any frame of the video through other frames. However, mismatches are prone to occur between the generated video frames, resulting in the inability to meet the continuity of the video frames, that is, temporal artifacts of the generated video. Given a set of video frames  $V = \{F_1, F_2, \dots, F_L\}$ , we define the method to determine

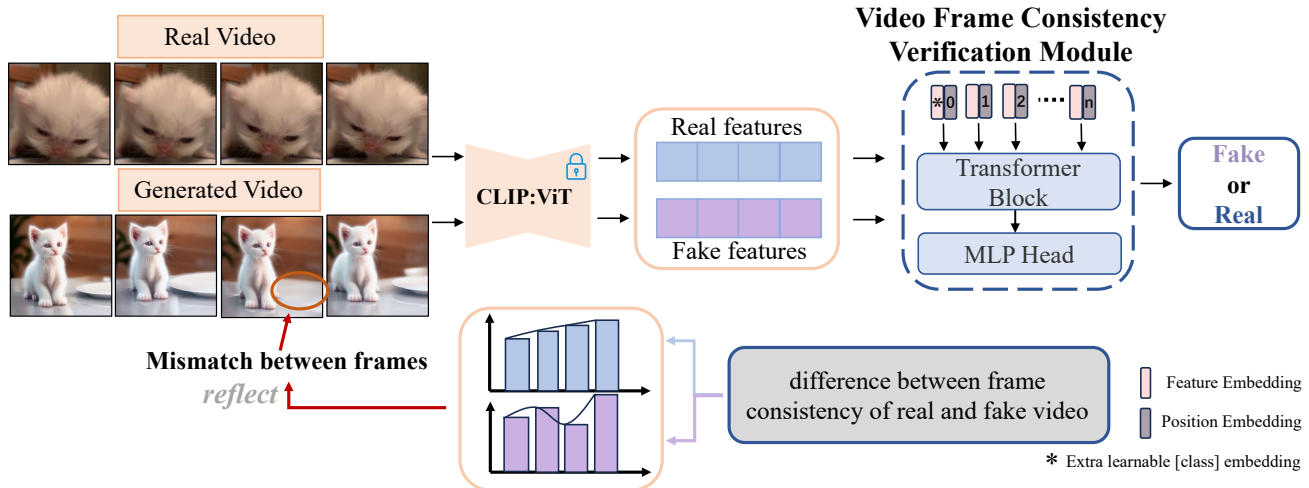


Figure 8. Overview of the DeCoF framework. We first get real video and generated video features by the pre-trained model CLIP:ViT, which is designed to eliminate the impact of spatial artifacts on capture temporal artifacts, and then a verification module consisting of two transformer layers and one MLP head is used to learn the differences between frame consistency of real and fake video.

the authenticity of a video based on its temporal artifacts as  $f(F_1, F_2, \dots, F_L) = y$ , where  $f$  is a particular function that measures the continuity between video frames,  $y \in Y = \{0, 1\}$  is the authenticity label of the video.

After analyzing the results of the above exploration, it appears that the detection model tends to learn spatial artifacts that are easy to capture but do not have generalization properties. **The difficulty lies in how to eliminate the impact of spatial artifacts on capturing temporal artifacts.**

Intuitively, if we can find a particular mapping function  $g$  with the following properties: The distance between frame mappings is negatively related to the image similarity, and the mapping function is insensitive to spatial artifacts. In fact, we choose ViT-L/14 (Dosovitskiy et al., 2020) trained for the task of image-language alignment as mapping function  $g$ , then by mapping the video frames  $F_i$  to  $g(F_i)$ , the decoupling of temporal artifacts and spatial artifacts can be achieved. As a result, the original problem can be expressed as  $f(g(F_1), g(F_2), \dots, g(F_L)) = y$ .

**Model framework.** In order to learn video frame consistency for capturing temporal artifacts, we design our detection with the Consistency of video Frames (DeCoF), in which the critical verification module consists of two transformer layers and an MLP head, As shown in Figure 8. More specifically, given a video input  $V$ , The frozen parameter image encoder (ViT-L/14) will extract the features of the video frames and generate a feature sequence  $S = \{g(F_1), g(F_2), \dots, g(F_L)\}$  with a shape of  $L * D$ , where  $D$  represents the dimension of each feature. Next, the position encoding and a learnable class embedding representing the classification output are prepended to the sequence  $S$  and then passed through a sequential module

composed of two layers of transformers. Finally, a classification header is appended to the transformer layer, resulting in a probability distribution over the target class, and we train our model via a simple cross-entropy loss.

In addition to decoupling temporal and spatial artifacts, our approach significantly reduces computational complexity and memory requirements since we only need to learn anomalies between video frame features. Overall, our approach is simple yet effective.

## 6. Experiments

In this section, we introduce the experiment setup and provide extensive experimental results to demonstrate the superiority of our approach.

### 6.1. Experimental Setup

**Data pre-processing.** We only train on a certain sub-dataset of GVF and test on the remaining sub-datasets to evaluate the generalization of the detector. We take eight frames of each video for training and testing and center-crop each frame according to its shortest side, then resize it to 224×224. During the training process, some data augmentation, such as Jpeg compression, random horizontal flipping, and Gaussian blur, are also used.

**Evaluation metrics.** Following previous methods (Wang et al., 2020; 2023b; Frank et al., 2020), we mainly report accuracy (ACC) and average precision (AP) in our experiments to evaluate the detectors. The threshold for computing accuracy is set to 0.5 following (Wang et al., 2020; 2023b). For image-based methods, we average frame-level predictions into corresponding video-level predictions.

Table 2. Comprehensive comparison of our method with previous detectors and spatiotemporal convolutional networks, including CNNDet, DIF, DIRE, Lgard, I3D, Slow, X3D and Mvit, were tested on our GVF dataset using the officially provided model. \* Denotes our retraining on a subset of generated video forensics with official code. We report ACC (%) and AP (%) (ACC and AP in the Table).

Method	Training dataset	Generate mode	Detection Level	Tested generate video models								Total Avg.	
				Text2Video-zero		Show1		ModelScope		ZeroScope		ACC	AP
				ACC	AP	ACC	AP	ACC	AP	ACC	AP		
CNNDet(0.5)	LSUN	ProGAN	Image	49.61	41.47	49.74	47.58	49.61	43.40	49.94	59.85	49.73	48.08
CNNDet(0.1)	LSUN	ProGAN	Image	49.93	46.38	50.06	46.72	50.19	42.97	50.06	55.27	50.06	47.84
DIF	SDV2	Diffusion	Image	35.10	47.96	45.90	53.42	31.40	46.91	27.50	46.59	34.98	48.72
DIRE	LSUN-B	Diffusion	Image	63.14	63.45	51.80	51.70	51.48	51.03	46.71	42.96	53.28	52.29
Lgard	LSUN	ProGAN	Image	53.09	64.78	59.70	68.42	40.21	38.87	47.94	51.80	50.24	55.97
CNNDet (0.5)*	Text2Video-zero	T2V	Image	98.64	99.97	51.93	61.64	51.54	68.91	54.96	72.51	64.27	75.76
CNNDet (0.1)*	Text2Video-zero	T2V	Image	96.84	99.99	53.93	60.99	55.34	68.87	60.69	73.80	66.70	75.91
Lgard*	Text2Video-zero	T2V	Image	98.45	100.00	56.19	78.91	51.03	66.30	54.64	75.93	65.08	80.29
DIRE*	Text2Video-zero	T2V	Image	99.17	99.99	49.93	56.74	52.83	77.58	51.28	67.12	63.30	75.36
I3D*	Text2Video-zero	T2V	Video	98.00	99.87	49.75	70.41	49.25	71.43	50.50	51.85	61.88	73.39
Slow*	Text2Video-zero	T2V	Video	93.30	99.48	50.48	52.09	50.59	49.43	49.41	37.29	60.95	59.57
X3D*	Text2Video-zero	T2V	Video	94.84	98.61	49.41	33.52	48.35	43.07	49.85	30.89	60.61	51.52
Mvit*	Text2Video-zero	T2V	Video	98.42	99.97	49.96	45.93	49.49	38.98	51.68	32.60	62.39	54.37
DeCoF	Text2Video-zero	T2V	Video	99.50	100.00	71.50	95.83	78.25	96.13	76.50	96.13	81.44	97.02
DeCoF	Show1	T2V	Video	98.50	99.77	97.00	99.33	90.25	97.96	93.75	99.08	<b>94.88</b>	<b>99.04</b>
DeCoF	ModelScope	T2V	Video	98.50	99.94	80.25	95.68	97.00	99.53	93.75	98.93	92.38	98.52
DeCoF	ZeroScope	T2V	Video	97.00	99.81	75.50	96.52	75.75	96.42	98.50	99.91	86.69	98.17

**Baseline.** (i) CNNDet (Wang et al., 2020) proposes a model for detecting images generated by CNN. Through a large amount of data enhancement, the model has generalization on various images generated by CNN. (ii) DIF (Sinita & Fried, 2023) proposes a few-shot learning method for image synthesis. (iii) DIRE (Wang et al., 2023b) proposes a new image representation method called Diffusion Reconstruction Error (DIRE), which measures the error between the input image and its reconstruction via a pre-trained diffusion model to detect images generated by diffusion models. (iv) Lgard (Tan et al., 2023) used a pre-trained CNN model as a transformation model to convert images into gradients and used these gradients to present generalized artifacts. (v) I3D (Carreira & Zisserman, 2017) introduce a new Inflated 3D ConvNet that is based on 2D ConvNet inflation. (vi) Slow (Feichtenhofer et al., 2019) proposed a dual-path model, but we only adopted the Slow Pathway, which is designed to capture the semantic information provided by a small number of sparse frames. (vii) X3D (Feichtenhofer, 2020) designed a smaller and lighter structure and expanded it in different dimensions to achieve a trade-off between efficiency and accuracy. (viii) Mvit (Fan et al., 2021) combines the basic idea of multiscale feature hierarchies with transformer models for video and image recognition.

## 6.2. Detailed Evaluation

We conduct comprehensive and challenging experiments to answer the following questions:

**Q1. How does our detector perform at detecting unseen**

### T2V models compared to previous detectors?

As mentioned in Section 5.2, we found that previous detectors exhibit extraordinary capabilities when detecting specific generative models but lack generalization when unseen generative models are present. In the table 2, we quantitatively evaluate CNNDet (Wang et al., 2020), DIF (Sinita & Fried, 2023), DIRE (Wang et al., 2023b), Lgard (Tan et al., 2023), using the pre-trained weights provided by the official repository. Although these detectors have surprising performance in detecting generated images, their performance drops significantly on the task of detecting generated videos, with both ACC and AP below 60%. As a result of retraining the above four detectors on the sub-dataset Text2Video-zero, their performance on specific video generation models greatly improved, but they still performed poorly for unseen generation models, and ACC and AP scores are still lower than 60%, and even the retrained spatiotemporal convolutional network displays similar results. On the contrary, compared with previous detectors, our generated video detection method has excellent generalization for various unseen generation models. Specifically, on the task of generating video detection, the ACC increased by 17.74% ~ 31.38% and the AP by 16.73% ~ 49.18%.

We also conducted cross-dataset evaluations. Table 2 shows that on the task of generating video detection, the ACC of the model trained on the other three data sets is much higher than that of the model trained on Text2Video-zero by 5.25% ~ 13.44%. This is because Text2Video-zero has the worst temporal continuity in all four T2V generation models.

**Q2. How does our detector maintain robustness against**

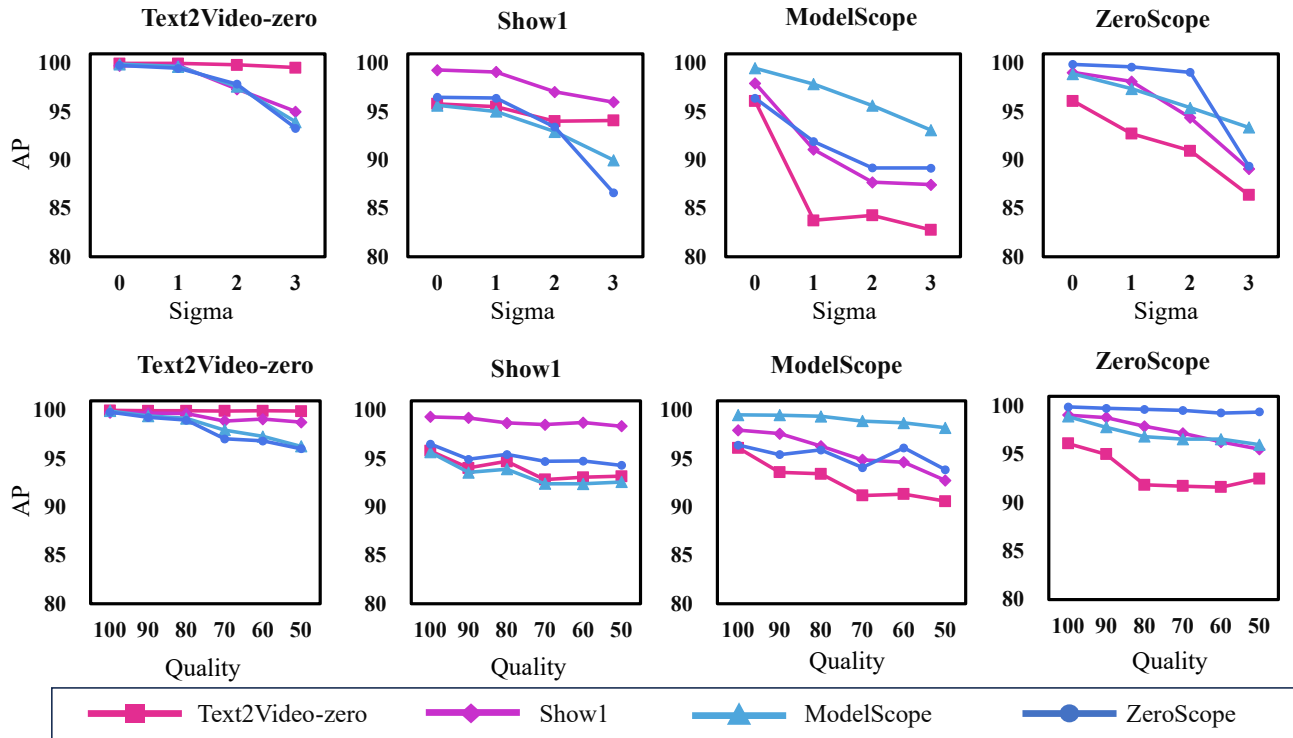


Figure 9. Robustness to unseen perturbations. The upper row represents the robustness of Gaussian blur, and the lower row represents the robustness of JPEG compression. We test the detectors trained on different sub-datasets (represented by different colors) on different sub-datasets and use the AP (%) report for robustness comparison.

Table 3. Performance of DeCoF on commercial generation models.

Training dataset	Tested generate video models				Total Avg.	
	Gen-2		Pika		ACC	AP
	ACC	AP	ACC	AP		
Text2Video-zero	99.49	100.00	99.49	99.98	99.49	99.99
Show1	98.46	99.96	98.46	99.85	98.46	99.91
ModelScope	98.97	99.99	96.89	99.73	97.93	99.86
ZeroScope	98.97	99.99	94.84	99.52	96.91	99.76

### noise and disturbances?

In practical detection scenarios, the robustness of the detector to unseen perturbations is also crucial. Here, we mainly focus on the impact of two perturbations on the detector: Gaussian blur and JPEG compression. The perturbations are added under three levels for Gaussian blur ( $\sigma = 1, 2, 3$ ) and five levels for JPEG compression (quality = 90, 80, 70, 60, 50). Figure 9 shows the performance of our model trained on different sub-datasets in the face of the above two perturbations. Although the model’s performance in the face of perturbations is inconsistent due to differences in training data sets, Our method remains effective under any degree of arbitrary perturbation, and the AP of models trained on any sub-dataset is greater than 80%.

### Q3. How does our detector perform on commercial generation models?

To further evaluate the effectiveness of our detection method, we constructed two additional test datasets using two well-known commercial proprietary T2V generation models, Pika (Pika, December 2023) and Gen-2 (Gen-2, December 2023). Based on the datasets generated by the four open-source T2V models shown in Table 3, the detector was trained on Text2Video-zero, Show1, ModelScope, and ZeroScope. When confronted with the commercial generation model, the detector achieved at least 94.84% ACC and 99.52% AP on Pika and at least 98.46% ACC and 99.96% AP on Gen-2, demonstrating the strong generalization capability of our model DeCoF for unseen T2V models. Even when trained on specific T2V models, the model is highly accurate in detecting newly generated video.

## 7. Conclusions and Future Work

The paper presents a groundbreaking investigation on generated video detection, with the goal of tackling the societal concern of validating the authenticity of video content. We construct the first public dataset for real and fake video detection, providing a solid benchmark for community re-

search. At the same time, we propose a simple yet effective detection model, which has proven its strong generalizability and robustness on multiple open-source and commercial closed-source models. We hope this study will inspire the creation and improvement of other detection technologies, providing new avenues for the development of authentic and reliable AIGC applications.

## 8. Impact Statements

Our research focuses on using Machine Learning to detect generated videos. We developed the DeCoF model and shared our dataset to support detecting synthetic videos. These works are crucial to protect digital content and prevent the spread of disinformation. Nevertheless, these tools have the potential to be misused, resulting in a rivalry between video generation and detection technology. We want to advocate for the ethical use of technology and foster research in the creation of tools for verifying media authenticity. We are confident that this will result in protecting the public from the harms of disinformation, improving the clarity and authenticity of information distribution, and ensuring the protection of personal privacy for individuals.

## References

- Agarwal, S., Farid, H., El-Gaaly, T., and Lim, S.-N. Detecting deep-fake videos from appearance and behavior. In *2020 IEEE international workshop on information forensics and security (WIFS)*, pp. 1–6. IEEE, 2020.
- Barni, M., Kallas, K., Nowroozi, E., and Tondi, B. Cnn detection of gan-generated face images based on cross-band co-occurrences analysis. In *2020 IEEE international workshop on information forensics and security (WIFS)*, pp. 1–6. IEEE, 2020.
- Barrett, C., Boyd, B., Bursztein, E., Carlini, N., Chen, B., Choi, J., Chowdhury, A. R., Christodorescu, M., Datta, A., Feizi, S., et al. Identifying and mitigating the security risks of generative ai. *Foundations and Trends® in Privacy and Security*, 6(1):1–52, 2023.
- Blattmann, A., Rombach, R., Ling, H., Dockhorn, T., Kim, S. W., Fidler, S., and Kreis, K. Align your latents: High-resolution video synthesis with latent diffusion models. In *Proceedings of the IEEE/CVF Conference on Computer Vision and Pattern Recognition*, pp. 22563–22575, 2023.
- Carreira, J. and Zisserman, A. Quo vadis, action recognition? a new model and the kinetics dataset. In *proceedings of the IEEE Conference on Computer Vision and Pattern Recognition*, pp. 6299–6308, 2017.
- Chen, D. and Dolan, W. B. Collecting highly parallel data for paraphrase evaluation. In *Proceedings of the 49th annual meeting of the association for computational linguistics: human language technologies*, pp. 190–200, 2011.
- Corvi, R., Cozzolino, D., Zingarini, G., Poggi, G., Nagano, K., and Verdoliva, L. On the detection of synthetic images generated by diffusion models. In *ICASSP 2023-2023 IEEE International Conference on Acoustics, Speech and Signal Processing (ICASSP)*, pp. 1–5. IEEE, 2023.
- Dosovitskiy, A., Beyer, L., Kolesnikov, A., Weissenborn, D., Zhai, X., Unterthiner, T., Dehghani, M., Minderer, M., Heigold, G., Gelly, S., et al. An image is worth 16x16 words: Transformers for image recognition at scale. *arXiv preprint arXiv:2010.11929*, 2020.
- Esser, P., Rombach, R., and Ommer, B. Taming transformers for high-resolution image synthesis. In *Proceedings of the IEEE/CVF conference on computer vision and pattern recognition*, pp. 12873–12883, 2021.
- Fan, H., Xiong, B., Mangalam, K., Li, Y., Yan, Z., Malik, J., and Feichtenhofer, C. Multiscale vision transformers. In *Proceedings of the IEEE/CVF international conference on computer vision*, pp. 6824–6835, 2021.
- Feichtenhofer, C. X3d: Expanding architectures for efficient video recognition. In *Proceedings of the IEEE/CVF conference on computer vision and pattern recognition*, pp. 203–213, 2020.
- Feichtenhofer, C., Fan, H., Malik, J., and He, K. Slowfast networks for video recognition. In *Proceedings of the IEEE/CVF international conference on computer vision*, pp. 6202–6211, 2019.
- Frank, J., Eisenhofer, T., Schönherr, L., Fischer, A., Kolossa, D., and Holz, T. Leveraging frequency analysis for deep fake image recognition. In *International conference on machine learning*, pp. 3247–3258. PMLR, 2020.
- Ge, S., Nah, S., Liu, G., Poon, T., Tao, A., Catanzaro, B., Jacobs, D., Huang, J.-B., Liu, M.-Y., and Balaji, Y. Preserve your own correlation: A noise prior for video diffusion models. In *Proceedings of the IEEE/CVF International Conference on Computer Vision*, pp. 22930–22941, 2023.
- Gen-2. Accessed january 17, 2024, December 2023. URL <https://research.runwayml.com/gen2>.
- Guarnera, L., Giudice, O., and Battiato, S. Deepfake detection by analyzing convolutional traces. In *Proceedings of the IEEE/CVF conference on computer vision and pattern recognition workshops*, pp. 666–667, 2020.
- Güera, D. and Delp, E. J. Deepfake video detection using recurrent neural networks. In *2018 15th IEEE international conference on advanced video and signal based surveillance (AVSS)*, pp. 1–6. IEEE, 2018.

- Guo, X., Liu, X., Ren, Z., Grosz, S., Masi, I., and Liu, X. Hierarchical fine-grained image forgery detection and localization. In *Proceedings of the IEEE/CVF Conference on Computer Vision and Pattern Recognition*, pp. 3155–3165, 2023.
- Haliassos, A., Vougioukas, K., Petridis, S., and Pantic, M. Lips don’t lie: A generalisable and robust approach to face forgery detection. In *Proceedings of the IEEE/CVF conference on computer vision and pattern recognition*, pp. 5039–5049, 2021.
- Ho, J., Jain, A., and Abbeel, P. Denoising diffusion probabilistic models. *Advances in neural information processing systems*, 33:6840–6851, 2020.
- Kawar, B., Zada, S., Lang, O., Tov, O., Chang, H., Dekel, T., Mosseri, I., and Irani, M. Imagic: Text-based real image editing with diffusion models. In *Proceedings of the IEEE/CVF Conference on Computer Vision and Pattern Recognition*, pp. 6007–6017, 2023.
- Khachatryan, L., Movsisyan, A., Tadevosyan, V., Henschel, R., Wang, Z., Navasardyan, S., and Shi, H. Text2video-zero: Text-to-image diffusion models are zero-shot video generators. *arXiv preprint arXiv:2303.13439*, 2023.
- Li, L., Bao, J., Zhang, T., Yang, H., Chen, D., Wen, F., and Guo, B. Face x-ray for more general face forgery detection. In *Proceedings of the IEEE/CVF conference on computer vision and pattern recognition*, pp. 5001–5010, 2020.
- Liu, Y., Li, L., Ren, S., Gao, R., Li, S., Chen, S., Sun, X., and Hou, L. Fetv: A benchmark for fine-grained evaluation of open-domain text-to-video generation. In *Thirty-seventh Conference on Neural Information Processing Systems Datasets and Benchmarks Track*, 2023.
- Masi, I., Killekar, A., Mascarenhas, R. M., Gurudatt, S. P., and AbdAlmageed, W. Two-branch recurrent network for isolating deepfakes in videos. In *Computer Vision–ECCV 2020: 16th European Conference, Glasgow, UK, August 23–28, 2020, Proceedings, Part VII 16*, pp. 667–684. Springer, 2020.
- McCloskey, S. and Albright, M. Detecting gan-generated imagery using saturation cues. In *2019 IEEE international conference on image processing (ICIP)*, pp. 4584–4588. IEEE, 2019.
- Nichol, A. Q. and Dhariwal, P. Improved denoising diffusion probabilistic models. In *International Conference on Machine Learning*, pp. 8162–8171. PMLR, 2021.
- Ojha, U., Li, Y., and Lee, Y. J. Towards universal fake image detectors that generalize across generative models. In *Proceedings of the IEEE/CVF Conference on Computer Vision and Pattern Recognition*, pp. 24480–24489, 2023.
- Parmar, G., Kumar Singh, K., Zhang, R., Li, Y., Lu, J., and Zhu, J.-Y. Zero-shot image-to-image translation. In *ACM SIGGRAPH 2023 Conference Proceedings*, pp. 1–11, 2023.
- Peebles, W. and Xie, S. Scalable diffusion models with transformers. In *Proceedings of the IEEE/CVF International Conference on Computer Vision*, pp. 4195–4205, 2023.
- Pika. Accessed january 17, 2024, December 2023. URL <https://www.pika.art/>.
- Ramesh, A., Dhariwal, P., Nichol, A., Chu, C., and Chen, M. Hierarchical text-conditional image generation with clip latents. *arXiv preprint arXiv:2204.06125*, 1(2):3, 2022.
- Rombach, R., Blattmann, A., Lorenz, D., Esser, P., and Ommer, B. High-resolution image synthesis with latent diffusion models. In *Proceedings of the IEEE/CVF conference on computer vision and pattern recognition*, pp. 10684–10695, 2022.
- Sha, Z., Li, Z., Yu, N., and Zhang, Y. De-fake: Detection and attribution of fake images generated by text-to-image generation models. In *Proceedings of the 2023 ACM SIGSAC Conference on Computer and Communications Security*, pp. 3418–3432, 2023.
- Sharma, D. K., Singh, B., Agarwal, S., Garg, L., Kim, C., and Jung, K.-H. A survey of detection and mitigation for fake images on social media platforms. *Applied Sciences*, 13(19):10980, 2023.
- Shiohara, K. and Yamasaki, T. Detecting deepfakes with self-blended images. In *Proceedings of the IEEE/CVF Conference on Computer Vision and Pattern Recognition*, pp. 18720–18729, 2022.
- Singer, U., Polyak, A., Hayes, T., Yin, X., An, J., Zhang, S., Hu, Q., Yang, H., Ashual, O., Gafni, O., et al. Make-a-video: Text-to-video generation without text-video data. *arXiv preprint arXiv:2209.14792*, 2022.
- Sinitisa, S. and Fried, O. Deep image fingerprint: Accurate and low budget synthetic image detector. *arXiv preprint arXiv:2303.10762*, 2023.
- Song, J., Meng, C., and Ermon, S. Denoising diffusion implicit models. In *International Conference on Learning Representations*, 2020.
- Sterling., S. zeroscope-v2 accessed january 17, 2024, June 2023. URL [https://huggingface.co/cerspense/zeroscope\\_v2\\_576w](https://huggingface.co/cerspense/zeroscope_v2_576w).
- Tan, C., Zhao, Y., Wei, S., Gu, G., and Wei, Y. Learning on gradients: Generalized artifacts representation for

- gan-generated images detection. In *Proceedings of the IEEE/CVF Conference on Computer Vision and Pattern Recognition*, pp. 12105–12114, 2023.
- Van der Maaten, L. and Hinton, G. Visualizing data using t-sne. *Journal of machine learning research*, 9(11), 2008.
- Vaswani, A., Shazeer, N., Parmar, N., Uszkoreit, J., Jones, L., Gomez, A. N., Kaiser, Ł., and Polosukhin, I. Attention is all you need. *Advances in neural information processing systems*, 30, 2017.
- Wang, J., Yuan, H., Chen, D., Zhang, Y., Wang, X., and Zhang, S. Modelscope text-to-video technical report. *arXiv preprint arXiv:2308.06571*, 2023a.
- Wang, S.-Y., Wang, O., Zhang, R., Owens, A., and Efros, A. A. Cnn-generated images are surprisingly easy to spot... for now. In *Proceedings of the IEEE/CVF conference on computer vision and pattern recognition*, pp. 8695–8704, 2020.
- Wang, Z., Bao, J., Zhou, W., Wang, W., Hu, H., Chen, H., and Li, H. Dire for diffusion-generated image detection. *arXiv preprint arXiv:2303.09295*, 2023b.
- Wang, Z., Bao, J., Zhou, W., Wang, W., and Li, H. Alt-freezing for more general video face forgery detection. In *Proceedings of the IEEE/CVF Conference on Computer Vision and Pattern Recognition*, pp. 4129–4138, 2023c.
- Xu, J., Mei, T., Yao, T., and Rui, Y. Msr-vtt: A large video description dataset for bridging video and language. In *Proceedings of the IEEE conference on computer vision and pattern recognition*, pp. 5288–5296, 2016.
- Zhang, D. J., Wu, J. Z., Liu, J.-W., Zhao, R., Ran, L., Gu, Y., Gao, D., and Shou, M. Z. Show-1: Marrying pixel and latent diffusion models for text-to-video generation. *arXiv preprint arXiv:2309.15818*, 2023.
- Zhang, X., Karaman, S., and Chang, S.-F. Detecting and simulating artifacts in gan fake images. In *2019 IEEE international workshop on information forensics and security (WIFS)*, pp. 1–6. IEEE, 2019.
- Zhao, H., Zhou, W., Chen, D., Wei, T., Zhang, W., and Yu, N. Multi-attentional deepfake detection. In *Proceedings of the IEEE/CVF conference on computer vision and pattern recognition*, pp. 2185–2194, 2021a.
- Zhao, T., Xu, X., Xu, M., Ding, H., Xiong, Y., and Xia, W. Learning self-consistency for deepfake detection. In *Proceedings of the IEEE/CVF international conference on computer vision*, pp. 15023–15033, 2021b.

---

## Supplementary Material

---

This supplementary material provides:

- The code is released at <https://anonymous.4open.science/r/DeCoF-8394>.
- Sec. A: A detailed description of dataset construction, including dataset structure diagrams, as well as specific examples of prompts and videos.
- Sec. B : Various parameter details for model training, hyperparameter settings, etc.
- Sec. C : The impact of selecting different mapping functions.
- Sec. D : More visual examples.

### A. Generated Video Forensics Dataset

#### A.1. Dataset Composition

The following section provides a more detailed description of how the generated video forensics dataset was constructed and evaluated. The entire GVF dataset is generated in two steps:

1) Selection of prompts and real videos: The prompts and real videos of the GVF dataset come from existing open-domain text-to-video datasets: MSVD (Chen & Dolan, 2011) and MSR-VTT (Xu et al., 2016) datasets. When selecting samples, we followed the work of FETV (Liu et al., 2023), Considering the collection of prompts from the above four aspects to simulate the sample distribution in real scenarios. More specifically, in the work of FETV, they classify each prompt controlling video generation from two aspects: the main content it describes and the attributes it controls during video generation. The spatial major content of the prompt can be divided into people, animals, plants, food, vehicles, buildings, artifacts, scenery, and illustrations. The corresponding spatial attribute controls are divided into quantity, color, and camera view. Likewise, the major contents and attribute controls of temporal are actions, kinetic motions, light change, and fluid motions, respectively, motion direction, speed, and event sequence.

2) Selection of generation models: Although there are many high-quality generative models on the market, we do not want to choose the best. On the contrary, we have selected four generative models with their advantages, aiming to simulate the crises we are encountering in real life: a large number of Generative models appear, how

do we deal with the problems caused by invisible generative models? In the end, the four most representative generative models were selected as our generative models: **Text2Video-zero** (Khachatriyan et al., 2023), **ModelScopeT2V** (Wang et al., 2023a), **ZeroScope** (Sterling, June 2023), **Show1** (Zhang et al., 2023). At the same time, we also selected the two most popular models as the secret test dataset: Pika (Pika, December 2023) and Gen-2 (Gen-2, December 2023).

If divided by content, the *GenerateVideoForensics* data set  $D$  consists of 964 triples, which can be expressed as  $D = \{(R, P, F)^{(i)}\}_{i=1}^{964}$ ,  $R$  and  $P$  represent real videos and corresponding text prompts,  $F$  represents multiple fake videos generated by different generation models based on text prompts  $P$ . If divided by the generation model, the *GenerateVideoForensics* data set can be divided into four sub-datasets: Text2Video-zero, ModelScopeT2V, ZeroScope, and SHOW-1. Each sub-dataset consists of 964 new triples, which can be expressed as  $D = \{(R, P, f)^{(i)}\}_{i=1}^{964}$ ,  $R$  and  $P$  represent the real video and the corresponding text prompt, and  $f$  represents the fake video generated by the specific generation model represented by the name of the current sub-dataset based on the text prompt  $P$ .

#### A.2. Dataset Evaluation

As part of this research, we present a comprehensive analysis of the GVF dataset, which includes an analysis of the attribute statistics of prompts, as well as an assessment of the different generation models in terms of the spatial content, spatial attributes, temporal content, and temporal attributes according to the FETV (Liu et al., 2023).

**Attribute statistics of prompts.** From the four aspects mentioned before, the main content of space and time and the main attributes of space and time, we provide attribute statistics of prompts of the data set. As the figure 10 shows, the various attributes of prompts are different because one prompt may have multiple attributes at the same time. At the same time, different attributes have different difficulties in generating videos, and the harm they cause in a trust crisis is also different. You may ask why time main content and time attributes are so rare. In fact, not every prompt in the MSVD and MSR-VTT datasets has a time description, and we only ensure the existence of this type of prompt in the data set. Here, we also provide some specific examples of prompts, As shown in the table 4.

Table 4. **Some examples of prompts.** Each prompt is composed of a random combination of four attributes: main content of time, main attributes of time, main content of space, and main attributes of space. Here we list some examples of prompts, red for content and blue for attributes.

	Main content	Attribute control	Example
Spatial	People	Quantity	four friends are driving in the car
	Animals	Color	a white bird chirps and plays on a handmade staircase
	Plants	Camera View	a beautiful view of greenery and river from a top view
	Food	Color	in cup full of chocolate then we add yellow cream to it so yummy
Temporal	Actions	Event Order	a red-headed woman is shown walking and then sitting
	Actions	Speed	a man fastly cross the road by run and get in to the car
	Kinetic Motions	Motion Direction	the big black tractor is moving away from it s carrier
	Fluid Motions	Speed	a bucket of slime is quickly poured on top of a woman’s head

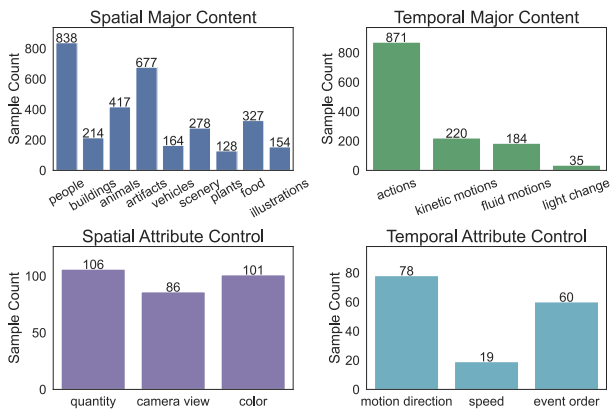


Figure 10. Data distribution over categories under the “major content” (upper) and “attribute control” (lower) aspects.

**Evaluation of different generation models.** Here, we present our assessment of four generation models according to the FETV standard (Liu et al., 2023). We assess the generated videos based on four perspectives: (i) Static quality focuses on the visual quality of single video frames. (ii) Temporal quality focuses on the temporal coherence of video frames. (iii) Overall alignment measures the overall alignment between a video and the given text prompt. (iv) Fine-grained alignment measures the video-text alignment regarding specific attributes.

As shown in figure 11, Regarding spatial categories, the performance quality of these four data sets varies, and the performance of the same data set differs significantly between the static quality and temporal quality levels. The videos that include people, animals, and vehicles have poor spatial quality, but the videos that include plants, scenery, and natural items have greater spatial quality. The reason behind this is that the videos in the first three categories contain numerous high-frequency intricacies, such as face and finger, which are more difficult to comprehend com-

pared to the low-frequency information found in the final two categories, such as water and clouds.

In terms of static quality, Text2Video-zero performs well but performs poorly in terms of temporal quality. Text2Video-zero inherited the ability to generate images from Stable Diffusion, but it lacks temporal coherence in its videos due to the lack of video training. SHOW-1 is second only to Text2Video-zero in terms of static quality, and its temporal quality is also superior. In comparison to ModelScopeT2V, ZeroScope is inferior to ModelScope in temporal quality but performs worse in static quality. The reason for this may be that ZeroScope has been primarily designed for videos with a 16:9 aspect ratio and without watermarks, rather than focusing on improving visual quality and aligning video text.

It is important to note that while the four models have better control over color and camera view, they do not perform as well when it comes to accurately controlling attributes such as quantity, motion direction, and order of the events. In terms of speed and motion direction attribute control, ModelScope and ZeroScope are particularly promising, whereas Text2Video-zero demonstrates poor performance.

On different attributes of the four models, fine alignment and global alignment perform similarly, although there are some exceptions. This is due to the fact that other properties may have an effect on the overall alignment. Therefore, it is more accurate to assess controllability using fine alignment when examining a specific attribute, whereas global alignment is a reasonable approximation.

## B. Parameter Description

In this section, we provide a detailed description of various parameters of the experiment, including the hyperparameters of the model and the details of its training.

**Training details.** During the training process, we only train

on one sub-dataset of the GVF dataset and test on the other sub-datasets. The numbers of the training set, validation set, and test set are 771, 97, and 96, respectively. We freeze the parameters of CLIP:ViT (Dosovitskiy et al., 2020), making it a pure mapping function, and only train our model using the SGD optimizer with an initial learning rate of 0.001 and a momentum coefficient of 0.9.

**Data pre-processing.** All the following experiments are performed on our GVF dataset. In order to better detect the videos generated by the unseen generate model, we only train the model on the sub-dataset text2video-zero and test on the remaining three sub-datasets Show1 (Zhang et al., 2023), ModelScope (Wang et al., 2023a) and ZeroScope (Sterling., June 2023) Since the resolution and length of the videos generated by the four generative models are inconsistent, We take eight frames of each video for training and testing and center-crop each frame according to its shortest side, then resize it to  $224 \times 224$ . During the training process, we first resized the image to  $256 \times 256$  according to bilinear interpolation and then randomly cropped with the size of  $224 \times 224$ . Some data augmentation, such as Jpeg compression, random horizontal flipping, and Gaussian blur, are also used.

**Model hyperparameters.** Our model consists of two layers of transformer and an MLP head is an adaptation of the sequence to sequence transformer, where the dimension and feature dimension of MLP is 768, path\_size is 32, the dropout parameter is 0.1, and the number of attention heads is 4.

### C. Different Mapping Functions

In this section, we examine the impact of different mapping functions.

The mapping function should have two properties. One is that the distance between features in the feature space is inversely proportional to the similarity between images, and the other is that it is insensitive to spatial artifacts. The second requirement is easy to implement as long as the mapping function is not used to train the fake content detection task. For the first requirement, we explored several different mapping functions, as shown in the table 5.

First, we discussed the two different tasks of ImageNet and CLIP. Interestingly, the encoder trained on ImageNet caused this problem not to converge. We considered two reasons: one is the size of the training data, and the other is Due to the difference in the task itself; we do not want the model to classify images into specific items or biological categories but rather cluster similar images. At the same time, we compared the impact of different model frameworks. Due to issues such as the number of model parameters, Resnet trained on the CLIP task is not suitable as a mapping func-

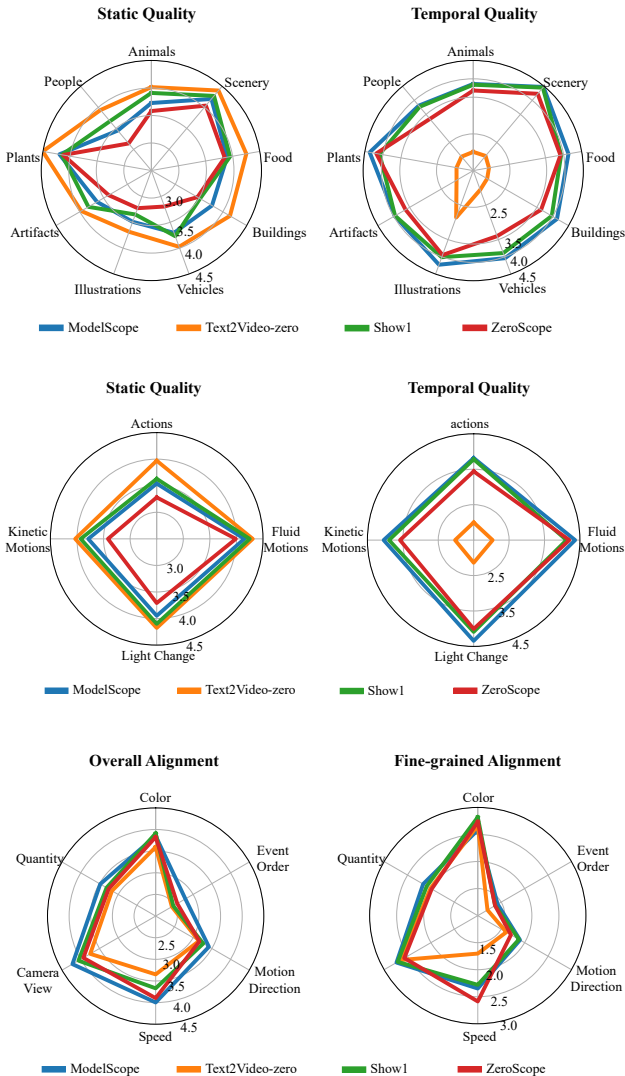


Figure 11. The manual evaluation provided results across major static and temporal contents and attributes to control video-text alignment.

Table 5. A comparison of the impact of different mapping functions.

Mapping Function	Pretrain Tasks	Tested generate video models								TotalAvg.	
		Text2Video-zero		Show1		ModelScope		ZeroScopre		ACC	AP
		ACC	AP	ACC	AP	ACC	AP	ACC	AP		
ViT-L/14	CLIP	99.50	100.00	71.50	95.83	78.25	96.13	76.50	96.13	81.44	97.02
Resnet50	CLIP	96.92	99.82	52.60	80.66	57.22	80.19	50.00	67.65	64.19	82.08
ViT-B/16	ImageNet	-	-	-	-	-	-	-	-	-	-
Resnet50	ImageNet	-	-	-	-	-	-	-	-	-	-

tion. Overall, the mapping function largely determines the effectiveness of our approach.

#### D. More Visual Examples

Here, we provide more examples of generated videos. Figures 12 to Figures 15 are examples of real videos and generated videos corresponding to prompts.

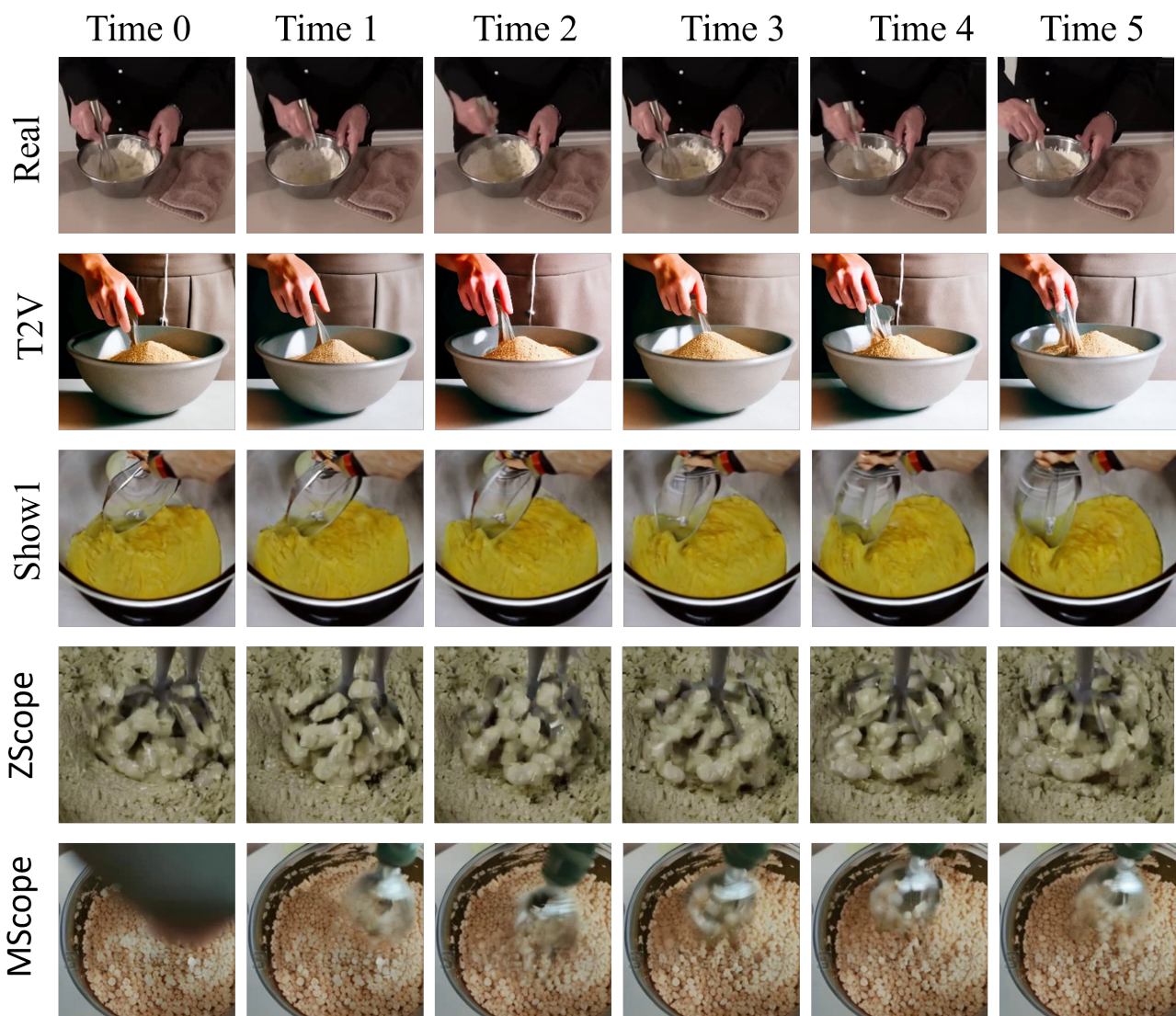


Figure 12. Real videos and videos generated by four generation models according to prompt: **A person mixing ingredients in a mixing bowl.**

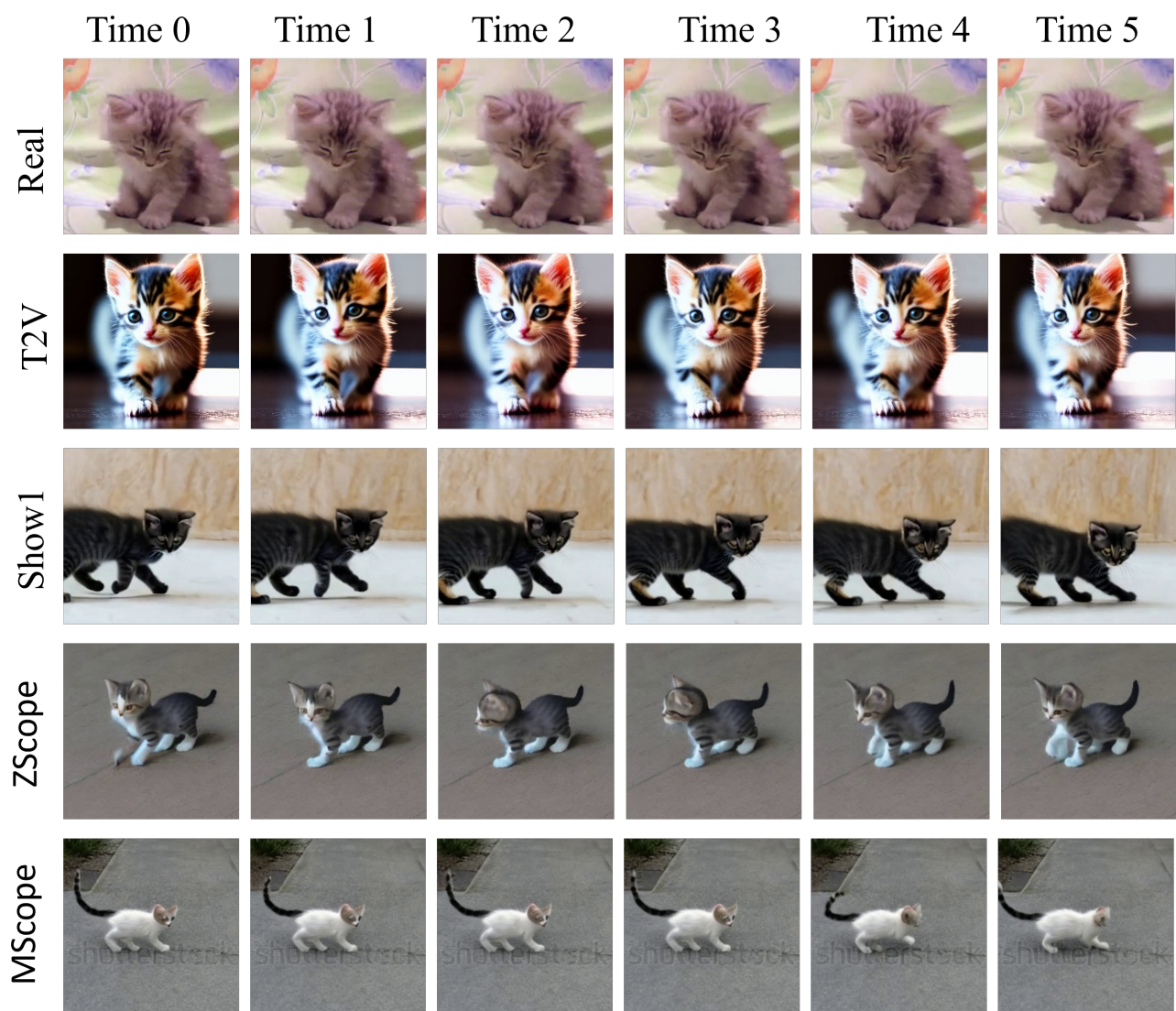


Figure 13. Real videos and videos generated by four generation models according to prompt: **A kitten moves about.**

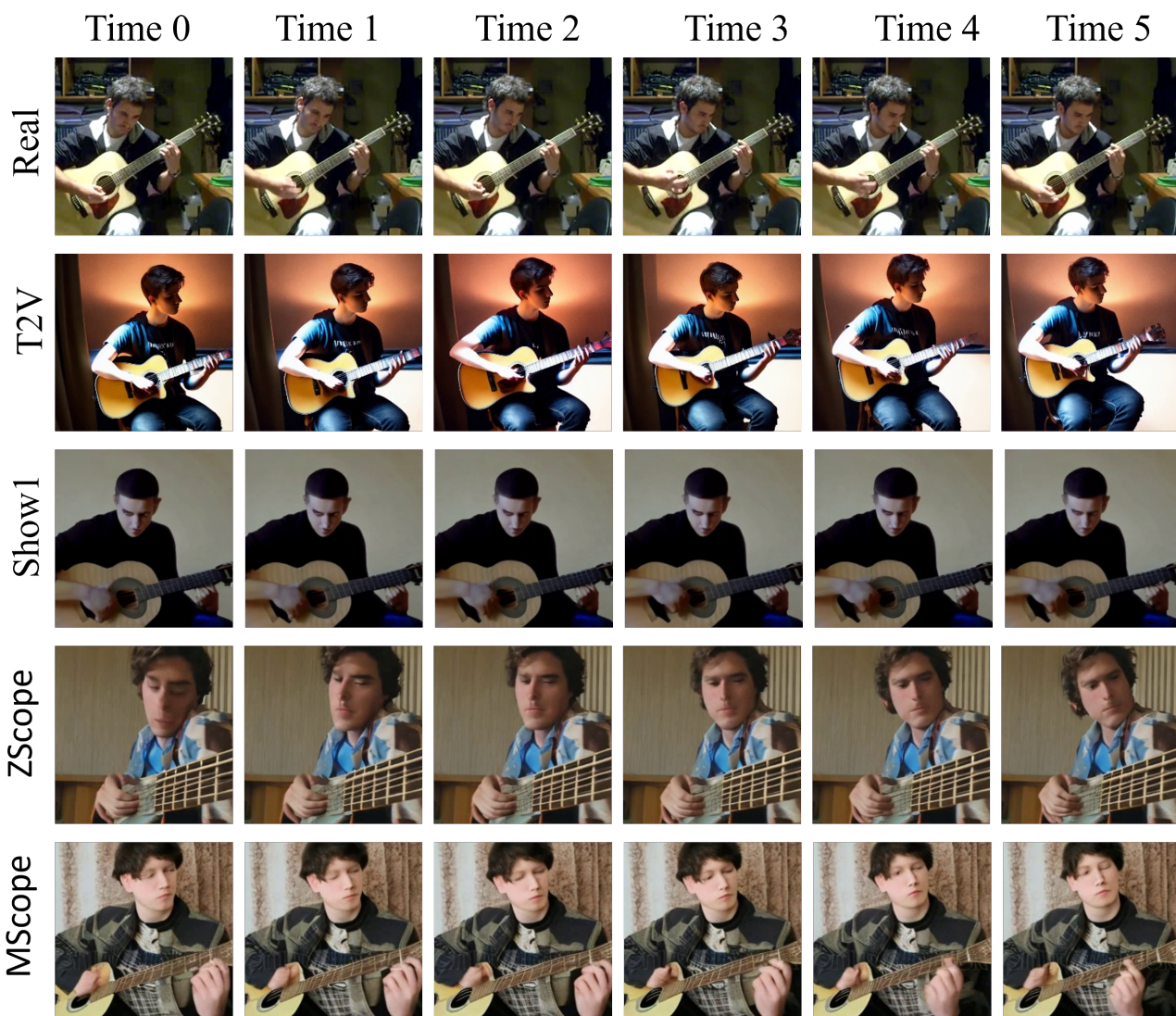


Figure 14. Real videos and videos generated by four generation models according to prompt: **A young man is seated and playing a guitar.**



Figure 15. Real videos and videos generated by four generation models according to prompt: **A boy rides a bike on a fence.**